Ernst & Sohn A Wiley Brand

Structural Concrete

POST-CRACKING RESIDUAL STRENGTHS OF FIBRE-REINFORCED HIGH PERFORMANCE CONCRETE AFTER CYCLIC LOADING

Journal:	*Structural Concrete*
Manuscript ID	Draft
Wiley - Manuscript type:	Technical Paper
Date Submitted by the Author:	n/a
Complete List of Authors:	Gonzlaez, Dorys; Universidad de Burgos Escuela Politecnica Superior, Civil Engineering Moradillo, Rosario; Universidad de Burgos Escuela Politecnica Superior, Civil Engineering Mínguez, Jesús; Universidad de Burgos Escuela Politecnica Superior, Civil Engineering Martínez, José; Universidad de Burgos Escuela Politecnica Superior, Civil Engineering VICENTE CABRERA, MIGUEL; Universidad de Burgos Escuela Politecnica Superior, Civil Engineering
Subject codes:	dynamic actions/earthquakes, analysis and design methods, testing | experiments, standards, regulations, guidelines, directives
Keywords:	Fatigue, High strength concrete, Fibre-reinforced high strength concrete, residual tension strength
Abstract:	This paper analyzes the variations in the residual tensile strength of steel fiber reinforced concretes following cyclic flexural loading, which causes a predefined level of damage. To do so, a total of 40 prismatic specimens were tested. The specimens were not notched, but had previously been subjected to pre-cracking. Doing so achieves a similar effect to notching, but with a much smaller radius around the edge of the fissure, which is therefore more vulnerable to fatigue. The results show that the damage provokes a progressive reduction in the residual traction strength. The study proposes two numerical expressions for the stress – crack width softening curves under tensile loads: an exponential formulation and a potential formulation. In both cases, the coefficients of both formulations depend on the damage that is applied. In addition, the proposal is to use fitted curves of the above-mentioned potential type.

POST-CRACKING RESIDUAL STRENGTHS OF FIBRE-REINFORCED HIGH PERFORMANCE CONCRETE AFTER CYCLIC LOADING.

Dorys C. González[1], Rosario Moradillo[2], Jesús Mínguez[3], José A. Martínez[4] and Miguel A. Vicente[5],

[1] Ph. D. Dorys C. González is Associate Professor of Concrete Technology at the Department of Civil Engineering, University of Burgos, Spain. c/Villadiego, s/n. 09001. Burgos. Spain. E-Mail: dgonzalez@ubu.es. Tfn: 0034-947-25.94.20. Fax: 0034-947-25.89.10. Corresponding Author.

[2] Ph. D. Candidate Rosario is Assistant Professor of Building Technology at the Department of Civil Engineering, University of Burgos, Spain. c/Villadiego, s/n. 09001. Burgos. Spain. E-Mail: rmoradi@ubu.es. Tfn: 0034-947-25.94.22. Fax: 0034-947-25.89.10.

[3] Ph. D. Jesús Mínguez is Assistant Professor of Concrete Technology at the Department of Civil Engineering, University of Burgos, Spain. c/Villadiego, s/n. 09001. Burgos. Spain. E-Mail: jminguez@ubu.es. Tfn: 0034-947-25.94.25. Fax: 0034-947-25.89.10.

[4] Ph. D. José A. Martínez is Associate Professor of Concrete Technology at the Department of Civil Engineering, University of Burgos, Spain. c/Villadiego, s/n. 09001. Burgos. Spain. E-Mail: jamartinez@ubu.es. Tfn: 0034-947-25.90.77. Fax: 0034-947-25.89.10.

[1] Ph. D. Miguel A. Vicente is Associate Professor of Structural Concrete and Bridge Technology at the Department of Civil Engineering, University of Burgos, Spain. c/Villadiego, s/n. 09001. E-Mail: mvicente@ubu.es. Tfn: 0034-947-25.94.23. Fax: 0034-947-25.89.10.

Number of words: 3308

Number of tables and figures: 28

Keywords: fatigue, high strength concrete, fibre-reinforced high strength concrete, residual tension strength.

31

ABSTRACT

This paper analyzes the variations in the residual tensile strength of steel fiber reinforced concretes following cyclic flexural loading, which causes a predefined level of damage. To do so, a total of 40 prismatic specimens were tested. The specimens were not notched, but had previously been subjected to pre-cracking. Doing so achieves a similar effect to notching, but with a much smaller radius around the edge of the fissure, which is therefore more vulnerable to fatigue. The results show that the damage provokes a progressive reduction in the residual traction strength. The study proposes two numerical expressions for the stress – crack width softening curves under tensile loads: an exponential formulation and a potential formulation. In both cases, the coefficients of both formulations depend on the damage that is applied. In addition, the proposal is to use fitted curves of the above-mentioned potential type.

1. INTRODUCTION

Fatigue in concrete may be understood as a process of mechanical weakening until failure. The cyclic loads cause the birth and the growth of microcracks inside the concrete mass. The macroscopic consequence of this phenomenon is a modification of its mechanical parameters.

Most research carried out over recent years have focused on obtaining predictions of the fatigue life, i.e., the number of cycles that the concrete element can withstand [1 to 21]. However, there are a few works that have focused on studying how the mechanical parameters of concrete are modified under cyclic loading [22 to 30].

Fibre-reinforced concretes (FRC) are widely used in construction (precast components of all types, pavements, etc.), because they offer the perfect combination of good mechanical behaviour and easy placement at work. These concretes are subjected to cyclic loading, in many common structural situations which cause efforts, mainly bending efforts. In addition, certain indirect actions, such as shrinkage and thermal variations, cause cracking. In this situation, the damage caused by the cyclic loads is especially focused on the cracked region.

According to the Model Code 2010 [31], the structural design of the FRC is based on the residual stress provided by the reinforcement fibres. In particular, the values of $f_{R,1}$ and $f_{R,3}$ are used in the formulation, defined as the residual strength values associated with crack openings of 0.5 and 2.5 mm, respectively.

In line with the above indications, the work of Gonzalez et al. (2014) may be highlighted, in which they show how cyclic flexural loads in FRC cause a progressive reduction in the residual strength under tension, $f_{R,j}$, in the case of elements with high fibre contents (2% in volume).

A correct design of the structural components of fibre-reinforced concrete subjected to cyclic loading should consider the minimum values of $f_{R,j}$, which correspond to the maximum number of cycles that the element will undergo during its service life. In other words, in the case of FRHSC structures subjected to the combined action of static loads and cyclic loads, validation of the structural safety under static loads should be done by taking into account the reduction of the mechanical capability of concrete, provoked by cyclic loading.

It is a similar situation, in some way, to pre and post-tensioned concrete. As deferred losses occur with pre- and post-tensioned concrete over time (due to concrete shrinkage and creep, and steel relaxation too). In consequence, validation of the structural safety is carried out taking into account the total time dependent losses.

This paper is focused on studying how the residual tensile strength of fibre-reinforced concrete varies in accordance with the damage provoked by cyclic loading.

2. EXPERIMENTAL PROGRAMM

The experimental study consisted of the analysis of the variation in the post-cracking residual strengths of C70/85 class FRC specimens according to Eurocode 2 [32], after undergoing three-point bending and cyclic loading tests. Once the cyclic loading test was finished, the specimens were subjected to static testing until failure, and then their post-cracking residual strengths were measured.

2.1 Materials

A total of 40 prismatic specimens 150x150x600 mm were casted. Table 1 shows the dosage of the mixture that was employed.

Ordinary Portland Cement, crushed limestone coarse and fine aggregates (maximum size 15 mm) were used. Hook-end steel fibres of 50 mm in length and 1.0 mm in diameter at 1% volume fraction were incorporated in the concrete. Superplasticizer Glenium 52 BASF and nanosilica MEYCO MS685 BASF were also used.

The specimens were cast in 2 batches, each batch consisting of twenty flexural test specimens and three cylindrical specimens of 150mm in diameter and 300 mm in length. The cylinders were used to determine their compressive strength at 28 days. Mixing was done in a rotary mixer and the fibres were gradually sprinkled into the drum by hand. The specimens were cured for 180 days in a curing room at a constant relative humidity of 100% and an ambient temperature of 20ºC. The specimens were then removed from the curing room and kept in the laboratory conditions until testing. All the specimens were, at least, 300 days-old when the testing campaign began. So, the possible strength increase during the fatigue test was avoided. The 28 days average compressive strength of the mix was 81.5 MPa.

.

2.2 Test

The test campaign consisted on four phases:

1. Precracking: In this phase, all forty prismatic specimens were subjected to a three-point static bending test until small cracks appeared.
2. Cyclic load tests to failure: These tests consisted of subjecting a total of twelve specimens to a three-point cyclic bending test to failure, to obtain the characteristic fatigue life of this fibre-reinforced concrete.
3. Cyclic load tests to a preset number of cycles: In the third phase, a total of twenty-one specimens underwent a three-point cyclic bending test up to a preset number of load cycles, with the purpose of causing controlled fatigue damage to the specimen.
4. Static tests after cyclic load: In the fourth phase, a total of twenty-eight specimens (twenty-one previously subjected to cyclic loading and another seven that had not been subjected to cyclic loads) underwent a three-point static bending test. In this way, variations in the residual tensile strength were determined with the fatigue damage.

The following provides a detailed description of each of the four research phases.

2.3 Pre-cracking Test

First, a static test was conducted, with the aim of create an initial crack (figure 1). To get it, the specimens were subjected to a three-point bending test, with a distance between bearings of 500 mm. The speed of the test was 0.05 mm/min.

During the test, the following parameters were measured: applied load and vertical deflection of the specimen. A MTS 244.4 dynamic actuator (MTS, Eden Prairie, Minnesota) was used, with a capacity of 500 kN under both tension and compression. The actuator was equipped with a load cell MTS 661.23 F-01 (MTS, Eden Prairie, Minnesota), with a range of 500 kN under both tension and compression and an error of below 1% of the range. For the measure of vertical deflection, two HBM WA-T displacement transducers (Hottinger Baldwin Messtechnik, Darmstadt, Germany) were used with a range of 50 mm and an accuracy of 0.01 mm.

The test was not until failure, but was stopped when the one of the two conditions was reached:

1. The applied load fell to 90% of the maximum load applied during the test.
2. Vertical deflection of the specimen was over 0.125 mm. In accordance with EN 14651:2005+A1:2007 [33], this figure would equate with the appearance of a crack greater than 0.1 mm.

This test is an alternative solution to notching, previously used by Gonzalez et al. (2014) [26] that provides much more realistic data. The presence of cracks substantially weakens the specimen and leaves it more vulnerable to fatigue. In real life, concrete elements subjected to cyclic loading are not notched, but may be pre-cracked (due, for example to shrinkage effects, among others). In these cases, the damage provoked by fatigue is concentrated around the cracks.

In accordance with the classic theory of fracture mechanisms in quasi-brittle materials (which includes concrete) [34], the stress at the edge of the crack depends on the radius of the edge of it. A notch provides a radius on the upper edge bigger than the one provide by a crack. In consequence, its stress concentration factor is lower and also the stress at the edge of the notch.

When concrete under cyclic loading is studied, this behaviour means that specimens with a previous crack are more vulnerable to cyclic loads than specimens with notches, given that, for the same value of cyclic loads, the cyclic stresses that appear in it are higher than those that appear in the notched specimens. In consequence, the damage provoked by cyclic loads is greater in specimens with previous fissures than in specimens with notches and their service life is shorter. [26].

2.4 Cyclic Load Tests to Failure

Subsequently, 12 of the previously cracked specimens were subjected to a cyclic test up until failure, with the purpose of obtaining the fatigue life of the concrete. In all cases, the maximum applied stress was 65% of its bending strength, obtained in the earlier pre-cracking tests; and the minimum applied stress was 5%. The test frequency was 6 Hz.

The result of this test campaign was the fatigue live of each specimen. Using a Weibull adjustment, the characteristic fatigue life was obtained, for a specific failure probability. In this case, it was considered that the characteristic fatigue life corresponded to a failure probability of 0.2 [12].

2.5 Cyclic Load Tests to a Preset Damage

The rest of the specimens, a total of 28, were subjected to a cyclic test up to a preset level of damage. In particular, the following levels of damage were studied: 0.0 (specimens not subjected to cyclic loading), 0.2, 0.8 and 0.9. From each series, a total of 7 specimens were tested. The damage was defined by the ratio between the number of cycles applied and the characteristic fatigue life (in this case, for a failure probability of 0.2 as explained before).

In all cases, the maximum applied stress was 65% of its bending strength, obtained in the pre-cracking tests; and the minimum applied stress was 5%. The test frequency was 6 Hz.

During the tests, two specimens broke before reaching the preset number of cycles.

2.6 Static Test after Cyclic Load

Once the cyclic load test to a preset damage were finished on the 26 surviving specimens, the performance of static tests up until failure (figures 2 and 3) were conducted. In the course of these tests, the stress – crack width softening curve for each of the specimens was obtained and the residual tension strength values ($f_{R,1}$, $f_{R,2}$, $f_{R,3}$ and $f_{R,4}$ respectively) were determined.

During this static test, the same parameters were measured as during the static pre-cracking tests (applied load and vertical deflection) as well as the crack opening. The width of the crack was measured using two axial extensometers MTS 624.12 F-24, with a total length of 15 mm and a precision of 0.01 mm.

The test was conducted in accordance with the specifications in standard EN14651:2005+A1:2007 [33].

These data make it possible to obtain expressions that correlate the values of residual traction strength with the damage.

Table 2 shows the identification of the specimens and the planning of the tests carried out. All the specimens underwent the pre-cracking test.

3. EXPERIMENTAL RESULTS

3.1 Pre-cracking Test

Tables 3 and 4 show the results of the proportionality limit on the pre-cracking tests $f_{L,pre}$, of the specimens subjected to pre-determined damage.

Figure 4 shows the distribution histogram of $f_{L,pre}$. Table 5 shows the basic statistical parameters of $f_{L,pre}$.

3.2 Cyclic Load Test to Failure

Table 6 shows the individual fatigue life values of each specimen, ordered from low to high.

By fitting the values to the Weibull distribution, it is possible to find the fatigue life for the different failure probabilities (figure 5).

Table 7 shows the characteristic fatigue life values, for different failure probabilities.

In this case, as indicated earlier, the value associated with a probability failure of 0.2 will be taken. In other words, from this point, the characteristic value of the fatigue life of our concrete will be considered to be 2,260 cycles.

3.2 Static Test after Cyclic Load

Table 8 shows the residual strength values ($f_{R,1}$, $f_{R,2}$, $f_{R,3}$ and $f_{R,4}$) in accordance with damage (D), of the specimens previously subjected to predetermined damage.

It is worth noting that specimens R-D0.8-3 and R-D0.9-5 collapsed before reaching the expected number of cycles.

On the basis of these data, the relative residual strength values may be determined (eq. 1):

$$f_{R,j,rel} = \frac{f_{R,j}}{f_{L,pre}} \qquad j \coloneqq 1\ to\ 4 \tag{2}$$

Relative strength gives a better understanding of the evolution of strength with damage. On the basis of the individual relative residual strengths values, the average and the characteristic values may be obtained, in accordance with a Gaussian distribution and a 95% probability of being exceeded. The average value is useful to understand the physical phenomenon and the characteristic value is used in the design of the structural elements.

Figures 6 to 8 show the relative individual, average and characteristic values, depending on the damage that is applied.

Figures 9 and 10 show a graph of the relative stress – crack width (w) in accordance with the damage applied to the specimen, both for the average value and the characteristic value.

The damage caused by the cyclic loads is, in this case, seen in a progressive reduction in the stiffness of the specimen. From a meso-structural point of view, cyclic loads cause cracking in the fibre-cement paste interface. This decrease means that bond between fibres and concrete will decrease and even, in some cases, lead to pulling out of fibres. Its consequence is a progressive reduction of the residual tension strength, both of the average value and of the characteristic value. This drop is equivalent to what happens with reinforcement bars, in the case of reinforced concrete [22 and 24].

A significant increase in the scatter of the results was also observed, which increased with the damage. This increase was to the detriment of the characteristic value, which was strongly reduced.

4. NUMERICAL ANALYSIS

There are few research works that propose empirical formulas for the estimation of the stress – crack width softening curve in fibre-reinforced concretes [35 to 40]. And far fewer analyse how cyclic loads affect the traction behaviour of fibre-reinforced concretes [41 and 42]. No research works are known by the authors that propose empirical formulas for the stress – crack width softening curve as a function of the damage caused by cyclic loads.

The following two adjusted curves are proposed: exponential and potential. Their details are set out below.

The proposal for an exponential curve in this document is similar to the one proposed in [35] and [36] according to the following expressions (eq. 3 and 4):

$$\sigma_{w,m,rel}(w) = exp(-a_m \cdot w) \tag{3}$$

$$\sigma_{w,k,rel}(w) = exp(-a_k \cdot w) \tag{4}$$

where the coefficients a_m, and a_k depend on the damage applied to the specimen. Equation 3 fits the average stress values, while equation 4 fits the characteristic values.

The proposal for a potential curve in this work is similar to the one proposed in [37] and [40], according to the following expressions (eq. 5 and 6):

$$\sigma_{w,m,rel}(w) = \frac{1}{1+\frac{w}{b_m}} \tag{5}$$

$$\sigma_{w,k,rel}(w) = \frac{1}{1+\frac{w}{b_k}} \tag{6}$$

where the coefficients b_m, and b_k depend on the damage applied to the specimen. Equation 5 fits the average stress values, while equation 6 fits the characteristic values.

Next a comparative study of both fitted formulas is conducted (figures 11 to 14).

As may be appreciated, the exponential function shows a better fit than the potential function. In table 9, the fitted values obtained in each case (figures 15 and 16) are shown.

In figure 15, the presence of three bounded areas may be perceived in the material. A first one, that runs from D=0.0 up to D=0.2 in which the increase of the parameters is quite significant. Following on, a second region is shown, which runs from D=0.2 to D=0.8 in which the curve presents a gentler slope. Finally, for damage values of over 0.8, the increase of the adjusted parameters was more significant.

Figure 16 shows an equivalent behaviour. Three regions may also be seen. In the first region, that runs from D=0.0 to D=0.2, the descent of the parameters is sharper. As from this level of damage and up until D=0.8, the fall is much gentler, rising once again as from D=0.8.

An equivalent behavioural pattern occurs with other concrete parameters when subjected to fatigue. For example, the identification of three regions is well documented in the analysis of variations in maximum deformation with the cyclic load, in the case of concrete elements under compression [43]. This same pattern was also identified in the case of the evolution of the modulus of elasticity of the concrete under cyclic loads [23, 28 and 29].

The following expressions a_m, a_k, b_m y b_k are proposed to adjust the values of expressions (eq. 7 a 10):

$$a_m(w) = a_{m,0} \cdot \frac{1}{1-D^{\alpha_m}} \tag{7}$$

$$a_k(w) = a_{k,0} \cdot \frac{1}{1-D^{\alpha_k}} \tag{8}$$

$$b_m(w) = b_{m,0} \cdot \left(1 - D^{\beta_m}\right) \tag{9}$$

$$b_k(w) = b_{k,0} \cdot \left(1 - D^{\beta_k}\right) \tag{10}$$

where $a_{m,0}$, $a_{k,0}$, $b_{m,0}$, $b_{k,0}$, α_m, α_k, β_m y β_k are the adjusted parameters.

In figures 17 and 18, the curves fitted to the parameters shown in table 6 are shown.

In table 10, the fitted values of equation parameters 7 to 10 are shown.

All the proposed equations are consistent with the physical behaviour that was observed. Both in the case of the exponential fitted parameters and the potential fitted parameters, it is found that when D=1, then $\sigma_{w,m,rel}$ and $\sigma_{w,k,rel}$ are equal to 0.

Incorporating equations 7 to 10 in equations 3 to 6, the following equations are found (eq. 11 to 14):

$$\sigma_{w,m,rel}(w) = exp\left(-a_{m,0} \cdot \frac{1}{1-D^{\alpha_m}} \cdot w\right) \tag{11}$$

$$\sigma_{w,k,rel}(w) = exp\left(-a_{k,0} \cdot \frac{1}{1-D^{\alpha_k}} \cdot w\right) \tag{12}$$

$$\sigma_{w,m,rel}(w) = \frac{1}{1+\frac{w}{b_{m,0} \cdot \left(1-D^{\beta_m}\right)}} \tag{13}$$

$$\sigma_{w,k,rel}(w) = \frac{1}{1+\frac{w}{b_{k,0} \cdot \left(1-D^{\beta_k}\right)}} \tag{14}$$

Particularizing the relative stress – crack width softening curves for the crack width values of 0.5, 1.5, 2.5 and 3.5 mm, the residual tension strength values are obtained (eq. 15 to 18):

$$f_{R,j,rel,m} = exp\left(-a_{m,0} \cdot \frac{1}{1-D^{\alpha_m}} \cdot w_j\right) \tag{15}$$

$$f_{R,j,rel,k} = exp\left(-a_{k,0} \cdot \frac{1}{1-D^{\alpha_k}} \cdot w_j\right) \tag{16}$$

$$f_{R,j,rel,m} = \frac{1}{1+\frac{w_j}{b_{m,0} \cdot \left(1-D^{\beta_m}\right)}} \tag{17}$$

$$f_{R,j,rel,k} = \frac{1}{1+\frac{w_j}{b_{k,0} \cdot \left(1-D^{\beta_k}\right)}} \tag{18}$$

Where w_j takes the values of 0.5, 1.5, 2.5 and 3.5 mm respectively.

Substituting equation 2 into equations 15 to 18, the expressions are obtained that permit the determination of the average and characteristic values of residual traction strength in accordance with the damage, both for an exponential fit and for a potential fit (eq. 19 to 22):

$$f_{R,j,m} = f_{L,pre} \cdot exp\left(-a_{m,0} \cdot \frac{1}{1-D^{\alpha_m}} \cdot w_j\right) \tag{19}$$

$$f_{R,j,k} = f_{L,pre} \cdot exp\left(-a_{k,0} \cdot \frac{1}{1-D^{\alpha_k}} \cdot w_j\right) \quad (20)$$

$$f_{R,j,m} = f_{L,pre} \cdot \frac{1}{1+\frac{w_j}{b_{m,0}\cdot\left(1-D^{\beta m}\right)}} \quad (21)$$

$$f_{R,j,k} = f_{L,pre} \cdot \frac{1}{1+\frac{w_j}{b_{k,0}\cdot\left(1-D^{\beta_k}\right)}} \quad (22)$$

These formulas propose an estimation of the values of residual tension strength in accordance with the damage. The adjustment factors, listed in table 6, were optimized for this research. Different fibre types and contents, as well as different cyclic load morphologies will yield different numeric values of the factors.

6. CONCLUSIONS

This paper shows the variation of the residual tension strength of FRHSC specimens previously subjected to pre-determined levels of damage. In the case of FRHSC structures subjected to the combined action of static and cyclic loading, the estimation of its structural safety under static loads should be determined by taking into account the reduction of its mechanical capability provoked by cyclic loading.

The main conclusions obtained in this work are as follows:

1. Cyclic loads cause a progressive reduction in the stiffness of the specimens, which conducts to a reduction in the residual tension strength. From a meso-structural point of view, cyclic loads provoke cracking in the fibre-cement paste interface, causing a reduction of fibre-concrete bond, which results in a reduction of the residual strength.
2. Two families of mathematical expressions are proposed to fit the stress – crack width softening curve; exponential adjustment and potential adjustment. The exponential expressions present, in general, better adjustment than the potential expressions.
3. The coefficients of the adjusted expressions correlate with damage. Its curves point to compartmentalization into three regions. It is a behavioural pattern that is repeated in many other concrete parameters when they correlate with the damage caused by cyclic loading (maximum deformation, modulus of elasticity, etc.).
4. Finally, empirical expressions are proposed that correlate residual tension strength with damage.

REFERENCES

[1]. Goel, S.; Singh, S.P.; Singh, P. (2012). "Flexural fatigue strength and failure probability of Self Compacting Fibre Reinforced Concrete beams". Engineering Structures, v 40, pp. 131-140.

[2]. Singh, S.P.; Sharma, U.K. (2007). “Flexural fatigue strength of steel fibrous concrete beams”. Advances in Structural Engineering, v 40(2), pp. 197-207.

[3]. Singh, S.P., Mohammadi, Y.; Kaushik, S.K. (2005). “Flexural fatigue analysis of steel fibrous concrete containing mixed fibers”. ACI Materials Journal, v 102(6), pp. 438-444.

[4]. Bajaj, V.; Singh, S.P.; Singh, A.P. et al (2012). “Flexural fatigue analysis of hybrid fibre-reinforced concrete”. Magazine of Concrete Research, v 64(4), pp. 361-373.

[5]. Singh, S.P.; Kaushik, S.K. (2000) “Flexural fatigue life distributions and failure probability of steel fibrous concrete”. ACI Materials Journal, v 97(6), pp. 658-667.

[6]. Mohammadi, Y.; Kaushik, S.K. (2005) “Flexural fatigue-life distributions of plain and fibrous concrete at various stress levels”. Journal of Materials in Civil Engineering, v 17(6), pp. 650-658.

[7]. Singh, S.P.; Kaushik, S.K. (2001). “Flexural fatigue analysis of steel fiber-reinforced concrete”. ACI Materials Journal, v 98(4), pp 306-312.

[8]. Johnston, C.D.; Zemp, R.W. (1991). “Flexural fatigue performance of steel fiber reinforced concrete. Influence of fiber content, aspect ratio and type”. ACI Materials Journal, v 88(4), pp. 374-383.

[9]. Plizzari, G.A.; Cangiano, S.; Cere, N. (2000). “Postpeak behavior of fiber-reinforced concrete under cyclic tensile loads”. ACI Materials Journal, v 97(2), pp. 182-192.

[10]. Naaman, A.E.; Hammoud H. (1998) “Fatigue Characteristics of High Performance Fiber-reinforced Concrete”. Cement and Concrete Composites, v 20, pp.353-363

[11]. Zhang B.; Wu K. (1997) “Residual fatigue strength and stiffness of ordinary concrete under bending” Cement and Concrete Research, v 27(1), pp. 115-126.

[12]. Graeff, A.G.; Pilakoutas, K.; Neocleous, K., et al (2012) “Fatigue resistance and cracking mechanism of concrete pavement reinforced with recycled steel fibres recovered from post-consumer tyres”. Engineering Structures, v 45, pp. 385-395.

[13]. Li, H.; Zhang, M.; Ou, J. (2007). “Flexural fatigue performance of concrete containing nano-particles for pavement”. International Journal of Fatigue, v 29(7), pp. 1292-1301.

[14]. Patel, P.A.; Desai, A.K.; Desai, J.A. (2013) “Evaluation of RC and SFRC exterior beam-column joint under cyclic loading for reduction in lateral reinforcement of the joint region”. Magazine of Concrete Research, v 65(7), pp. 405-414.

[15]. Zhang, Y.; Harries, K.A.; Yuan, W. (2013). "Experimental and numerical investigation of the seismic performance of hollow rectangular bridge piers constructed with and without steel fiber reinforced concrete". Engineering Structures, v 58, pp. 255-265.

[16]. Vasconez, R.M.; Naaman, A.E.; Wright, J.K. (1998) "Behavior of HPFRC connections for precast concrete frames under reversed cyclic loading". PCI Journal, v 43(6), pp. 58-71.

[17]. Filiatrault, A.; Ladicani, K.; Massicotte, B. (1994). "Seismic performance of code-designed fiber-reinforced concrete joints". ACI Structural Journal, v 91(5), pp. 564-571.

[18]. Shah A.; Abid, Ribakov Y. (2011) "Recent trends in steel fiber high-strength concrete". Materials and Design, v 32, pp. 4122-4151.

[19]. Naaman A.E.; Hammoud H. (1998) "Fatigue Characteristics of High Performance Fiber-reinforced Concrete". Cement and Concrete Composites, v 20, pp.353-363.

[20]. Hsu, T.T.C. (1981). "Fatigue of plain concrete". ACI J., v 78(4), pp 292-305.

[21]. Petkovic, G.; Lenschow, R.; Stemland, H.; Rosseland, S. (1990). "Fatigue of high-strength concrete". ACI Special Publication, v 121, pp. 505-526.

[22]. Bernardo, H.; Vicente, M.A.; González, D.C.; Martínez, J.F. (2015). "Efecto de las cargas cíclicas sobre la adherencia hormigón-acero en hormigones sumergidos". Hormigón y Acero, v 66(276).

[23]. Vicente, M.A.; González, D.C.; Mínguez, J.; Martínez, J.A. (2014). "Residual modulus of elasticity and máximum compressive strain in HSC and FRHSC after high-stress-level cyclic loading.". Structural Concrete, v. 15(2), pp. 210-218.

[24]. Bernardo, H.; Vicente, M.A.; González, D.C.; Martínez, J.F. (2014). "Cyclic bond testing of steel bars in high-performance underwater concrete". Structural Engineering International, v 24(1), pp. 37-44.

[25]. Vicente, M.A; González, D.C.; Martínez, J.A. (2014). "Mechanical Response of Partially Prestressed Precast Concrete I-Beams after High-Range Cyclic Loading." Pract. Period. Struct. Des. Constr., 10.1061/(ASCE)SC.1943-5576.0000225, 04014022.

[26]. González, D.C; Vicente, M.A.; Ahmad, S. (2014). "Effect of Cyclic Loading on the Residual Tensile Strength of Steel Fiber–Reinforced High-Strength Concrete." J. Mater. Civ. Eng., 10.1061/(ASCE)MT.1943-5533.0001200, 04014241.

[27]. Urban, S.; Strauss, A.; Macho, W.; Bergmeister, K.; Dehlinger, C. and Reiterer, M. "Zyklisch belastete Betonstrukturen. Robustheits- und Redundanzbetrachtungen zur Optimierung der Restnutzungsdauer (Concrete

structures under cyclic loading. Robustness and redundancy considerations for residual lifetime optimization) (In German)". Bautechnik, vol. 89, no 11, 2012,

[28]. Zanuy, C.; Albajar, L.; De la Fuente P. (2011). "The fatigue process of concrete and its structural influence," Materiales de Construcción, v 61(303), pp. 385-399.

[29]. Zanuy, C.; Albajar, L.; de la Fuente, P. (2009). "Sectional analysis of concrete structures under fatigue loading", ACI Struct. J., v 106(5), pp. 667-677.

[30]. Zhang, B.; Wu, K. (1997). "Residual fatigue strength and stiffness of ordinary concrete under bending" Cement and Concrete Research, v 27(1), pp. 115-126.

[31]. International Federation for Structural Concrete. (2010). "Model code for concrete structures." FIB Bulletin 65, Lausanne, Switzerland.

[32]. European Committee for Standardization (2004). "EUROCODE 2, Design of concrete structures". Eurocode2, Brussels, Belgium.

[33]. British Standards Institution. (2008). "Test method for metallic fiber concrete—Measuring the flexural tensile strength (limit of proportionality (LOP), residual)." EN 14651:2005+A1:2007, London.

[34]. Zongjin Li (2011). "Advanced Concrete Technology". John Wiley & Sons, Inc. ISBN: 9780470437438.

[35]. Gopalaratnam, V.S.; Shah, S.P. (1985) "Softening response of plain concrete in direct tension," ACI Journal, v 82(3), pp. 310–323.

[36]. Cedolin, L.; DeiPoli, S.; Iori, I. (1987) "Tensile behavior of concrete," Journal of Engineering Mechanics, ASCE, v 113(3), pp. 431–449.

[37]. Stang H.; Aarre, T. (1992). "Evaluation of crack width in FRC with conventional reinforcement". Cement & Concrete Composites, v 14, pp. 143-154.

[38]. Olesen, J.F. (2001). "Fictious crack propagation in fiber reinforced concrete beams". Journal of Engineering Mechanics, v 127(3), pp. 273-280.7

[39]. RILEM Technical Committees RILEM TC 162-TDF: Test and Design Methods for Steel Fibre Reinforced Concrete. (2002). "Design of steel fibre reinforced concrete using the σ-w method: principles and applications". Materials and Structures,, v 35(5), pp. 262-278.

[40]. Du, J.; Yon, J.H.; Hawkins, N.M.; Arakawa, K.; Kobayashi, A.S. (1992) "Fracture process zone for concrete for dynamic loading," ACI Materials Journal, v 89(3), pp. 252–258.

[41]. Zhang, J.; Li, V.C. (2004). "Simulation of crack propagation in fiber-reinforced concrete by fracture mechanics". Cement and Concrete Research, v. 34, pp. 333-339.

[42]. Cachim, P.B.; Figueiras, J.A.; Pereira, P.A.A. (2002). “Numerical modelling of fibre-reinforced concrete fatigue in bending”. International Journal of Fatigue, v. 24, pp. 381-387.

[43]. Holmen, J.O. (1982). “Fatigue of Concrete by Constant and Variable Amplitude Loading,” in Fatigue of Concrete Structures, ACI SP-75: 71-110.

TABLES AND FIGURES.

List of Tables:

List of Figures:

Figure 15: Parameters a_m and a_k versus damage.

Figure 16: Parameters b_m and b_k versus damage.

Figure 17: Parameters a_m and a_k versus damage. Power adjustment.

Figure 18: Parameters b_m and b_k versus damage. Power adjustment.

Table 1: Mix proportions

Cement (kg/m^3)	400
Water (kg/m^3)	125
Superplasticizer (kg/m^3)	14
Nanosilica (kg/m^3)	6
Fine aggregate (kg/m^3)	800
Coarse aggregate (kg/m^3)	1080
Fiber (% by volume)	1%

Table 2: Testing campaign.

SPECIMEN	TEST PROTOCOL	
R-F-1	Cyclic Load Tests to Failure	
R-F-2	Cyclic Load Tests to Failure	
R-F-3	Cyclic Load Tests to Failure	
R-F-4	Cyclic Load Tests to Failure	
R-F-5	Cyclic Load Tests to Failure	
R-F-6	Cyclic Load Tests to Failure	
R-F-7	Cyclic Load Tests to Failure	
R-F-8	Cyclic Load Tests to Failure	
R-F-9	Cyclic Load Tests to Failure	
R-F-10	Cyclic Load Tests to Failure	
R-F-11	Cyclic Load Tests to Failure	
R-F-12	Cyclic Load Tests to Failure	
R-D0.0-1	Cyclic Load Test to a Damage of 0.0	Static Test after Cyclic Load
R-D0.0-2	Cyclic Load Test to a Damage of 0.0	Static Test after Cyclic Load
R-D0.0-3	Cyclic Load Test to a Damage of 0.0	Static Test after Cyclic Load
R-D0.0-4	Cyclic Load Test to a Damage of 0.0	Static Test after Cyclic Load
R-D0.0-5	Cyclic Load Test to a Damage of 0.0	Static Test after Cyclic Load
R-D0.0-6	Cyclic Load Test to a Damage of 0.0	Static Test after Cyclic Load
R-D0.0-7	Cyclic Load Test to a Damage of 0.0	Static Test after Cyclic Load
R-D0.2-1	Cyclic Load Test to a Damage of 0.2	Static Test after Cyclic Load
R-D0.2-2	Cyclic Load Test to a Damage of 0.2	Static Test after Cyclic Load
R-D0.2-3	Cyclic Load Test to a Damage of 0.2	Static Test after Cyclic Load
R-D0.2-4	Cyclic Load Test to a Damage of 0.2	Static Test after Cyclic Load
R-D0.2-5	Cyclic Load Test to a Damage of 0.2	Static Test after Cyclic Load
R-D0.2-6	Cyclic Load Test to a Damage of 0.2	Static Test after Cyclic Load
R-D0.2-7	Cyclic Load Test to a Damage of 0.2	Static Test after Cyclic Load
R-D0.8-1	Cyclic Load Test to a Damage of 0.8	Static Test after Cyclic Load
R-D0.8-2	Cyclic Load Test to a Damage of 0.8	Static Test after Cyclic Load
R-D0.8-3	Cyclic Load Test to a Damage of 0.8	Static Test after Cyclic Load
R-D0.8-4	Cyclic Load Test to a Damage of 0.8	Static Test after Cyclic Load
R-D0.8-5	Cyclic Load Test to a Damage of 0.8	Static Test after Cyclic Load
R-D0.8-6	Cyclic Load Test to a Damage of 0.8	Static Test after Cyclic Load

R-D0.8-7	Cyclic Load Test to a Damage of 0.8	Static Test after Cyclic Load
R-D0.9-1	Cyclic Load Test to a Damage of 0.9	Static Test after Cyclic Load
R-D0.9-2	Cyclic Load Test to a Damage of 0.9	Static Test after Cyclic Load
R-D0.9-3	Cyclic Load Test to a Damage of 0.9	Static Test after Cyclic Load
R-D0.9-4	Cyclic Load Test to a Damage of 0.9	Static Test after Cyclic Load
R-D0.9-5	Cyclic Load Test to a Damage of 0.9	Static Test after Cyclic Load
R-D0.9-6	Cyclic Load Test to a Damage of 0.9	Static Test after Cyclic Load
R-D0.9-7	Cyclic Load Test to a Damage of 0.9	Static Test after Cyclic Load

Table 3: Results of the pre-cracking test (1).

SPECIMEN	$f_{L,pre}$ (MPa)
R-F-1	10.1
R-F-2	12.2
R-F-3	11.8
R-F-4	13.2
R-F-5	10.5
R-F-6	12.5
R-F-7	10.4
R-F-8	13.0
R-F-9	11.1
R-F-10	10.3
R-F-11	10.0
R-F-12	11.5

Table 4: Results of the pre-cracking test (2).

SPECIMEN	$f_{L,pre}$ (MPa)	SPECIMEN	$f_{L,pre}$ (MPa)	SPECIMEN	$f_{L,pre}$ (MPa)	SPECIMEN	$f_{L,pre}$ (MPa)
R-D0.0-1	10.8	R-D0.2-1	13.5	R-D0.8-1	12.4	R-D0.9-1	11.7
R-D0.0-2	16.3	R-D0.2-2	12.5	R-D0.8-2	14.6	R-D0.9-2	12.4
R-D0.0-3	14.2	R-D0.2-3	11.8	R-D0.8-3	9.3	R-D0.9-3	11.5
R-D0.0-4	10.5	R-D0.2-4	14.3	R-D0.8-4	15.7	R-D0.9-4	10.8
R-D0.0-5	10.9	R-D0.2-5	10.1	R-D0.8-5	12.4	R-D0.9-5	9.8
R-D0.0-6	10.1	R-D0.2-6	10.6	R-D0.8-6	12.7	R-D0.9-6	14.0
R-D0.0-7	11.4	R-D0.2-7	7.1	R-D0.8-7	10.3	R-D0.9-7	10.7

Table 5: Statistical analysis of the pre-cracking test.

μ (MPa)	σ	RSD	Skewness	Kurtosis
11.7	1.82	0.16	0.37	0.70

Table 6: Fatigue life of the specimens subjected to cyclic load test to failure, ordered from lower to higher.

Specimen	N
R-F-1	364
R-F-2	398

R-F-3	3,865
R-F-4	9,586
R-F-5	27,361
R-F-6	29,540
R-F-7	42,747
R-F-8	44,204
R-F-9	125,867
R-F-10	191,760
R-F-11	213,440
R-F-12	459,374

Table 7: Statistical fatigue life for different failure probabilities.

P_f	N
0.50	31,271
0.20	2,260
0.10	397
0.05	75

Table 8: Residual tensile strengths.

SPECIMEN	D	$f_{R,1}$ (MPa)	$f_{R,2}$ (MPa)	$f_{R,3}$ (MPa)	$f_{R,4}$ (MPa)
R-D0.0-1	0.0	9.7	6.4	4.6	3.5
R-D0.0-2	0.0	15.2	12.7	10.7	9.9
R-D0.0-3	0.0	13.1	10.4	8.4	7.1
R-D0.0-4	0.0	9.8	7.7	5.8	5.0
R-D0.0-5	0.0	9.5	7.4	6.6	5.2
R-D0.0-6	0.0	9.0	6.7	4.8	4.5
R-D0.0-7	0.0	10.2	6.6	4.9	3.6
R-D0.2-1	0.2	12.1	10.2	7.7	6.5
R-D0.2-2	0.2	10.9	8.4	6.8	4.5
R-D0.2-3	0.2	10.3	7.4	5.3	4.5
R-D0.2-4	0.2	11.6	7.8	5.7	4.3
R-D0.2-5	0.2	9.2	7.1	6.9	5.8
R-D0.2-6	0.2	9.2	5.6	4.6	3.2
R-D0.2-7	0.2	6.1	4.6	3.1	2.8
R-D0.8-1	0.8	9.7	6.4	5.1	3.2
R-D0.8-2	0.8	12.6	9.2	6.1	5.2
R-D0.8-3	0.8	--	--	--	--
R-D0.8-4	0.8	14.7	12.9	10.9	9.5
R-D0.8-5	0.8	10.8	7.2	5.7	4.7
R-D0.8-6	0.8	10.4	6.7	5.7	4.9
R-D0.8-7	0.8	8.5	6.3	3.1	2.0
R-D0.9-1	0.9	9.1	5.8	4.1	3.1
R-D0.9-2	0.9	8.8	5.7	4.0	3.4
R-D0.9-3	0.9	10.3	9.0	7.8	6.9
R-D0.9-4	0.9	10.1	6.2	3.9	2.4

R-D0.9-5	0.9	--	--	--	--
R-D0.9-6	0.9	11.2	9.4	7.1	3.7
R-D0.9-7	0.9	10.0	4.5	2.9	2.5

Table 9: Best-fit numerical values of parameters a_m, a_k, b_m and b_k.

Damage	a_m	a_k	b_m	b_k
0.00	0.2406	0.3720	3.0495	1.7622
0.20	0.2740	0.4478	2.5746	1.3754
0.80	0.3068	0.5651	2.2274	1.0203
0.90	0.3535	0.7339	1.8596	0.7265

Table 10: Best-fit numerical values of parameters $a_{m,0}$, $a_{k,0}$, $b_{m,0}$, $b_{k,0}$, α_m, α_k, β_m and β_k.

$a_{m,0}$	0.25
$a_{k,0}$	0.42
$b_{m,0}$	2.80
$b_{k,0}$	1.60
α_m	11.00
α_k	7.71
β_m	9.00
β_k	5.02

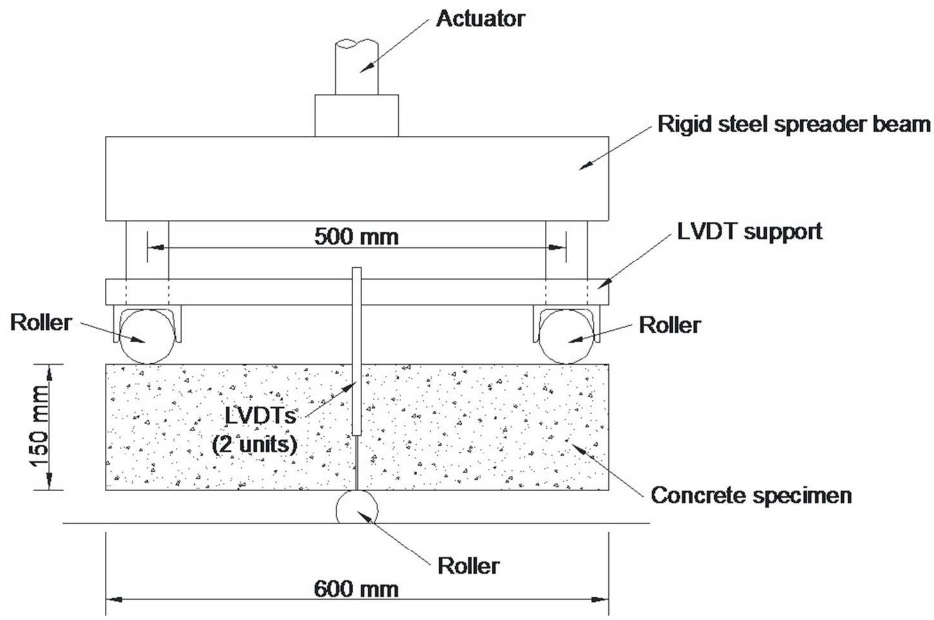

Figure 1: Schema of the pre-cracking testing
298x200mm (96 x 96 DPI)

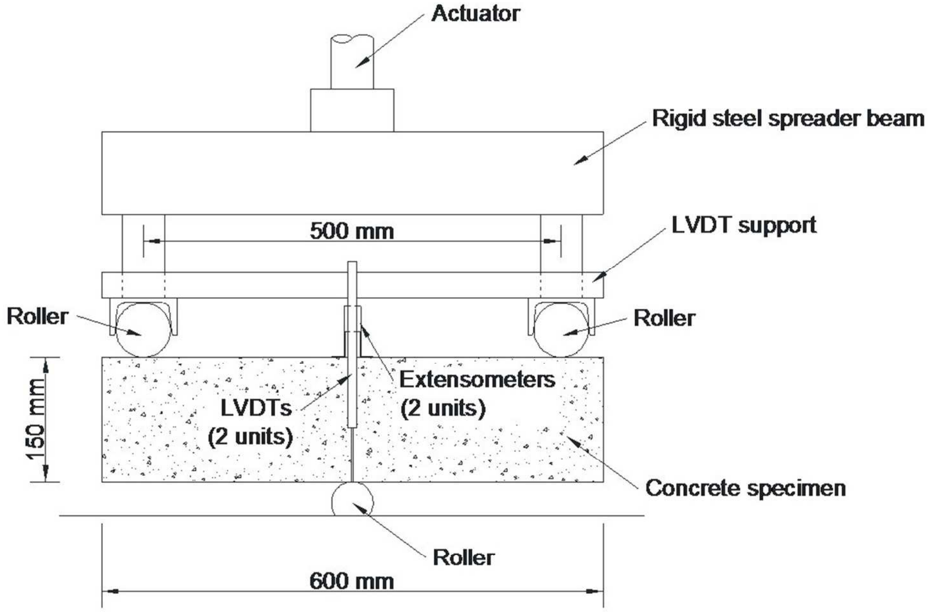

Figure 2: Schema of the static test after cyclic load
299x200mm (96 x 96 DPI)

Figure 3: Photo during the static test after cyclic load
281x211mm (120 x 120 DPI)

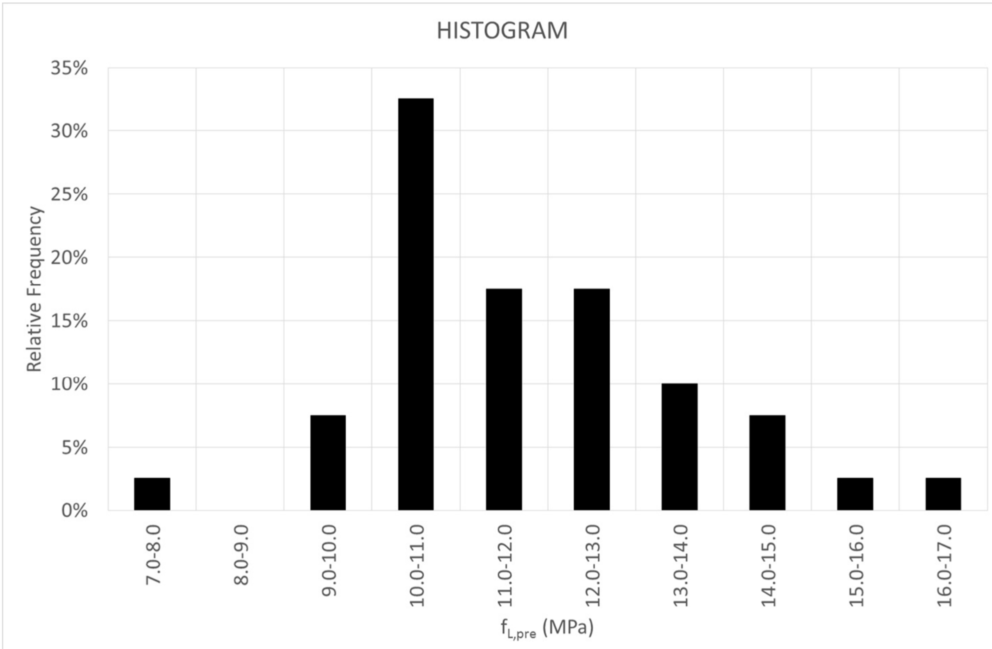

Figure 4: Histogram of statistical distribution of $f_{L,pre}$
310x202mm (120 x 120 DPI)

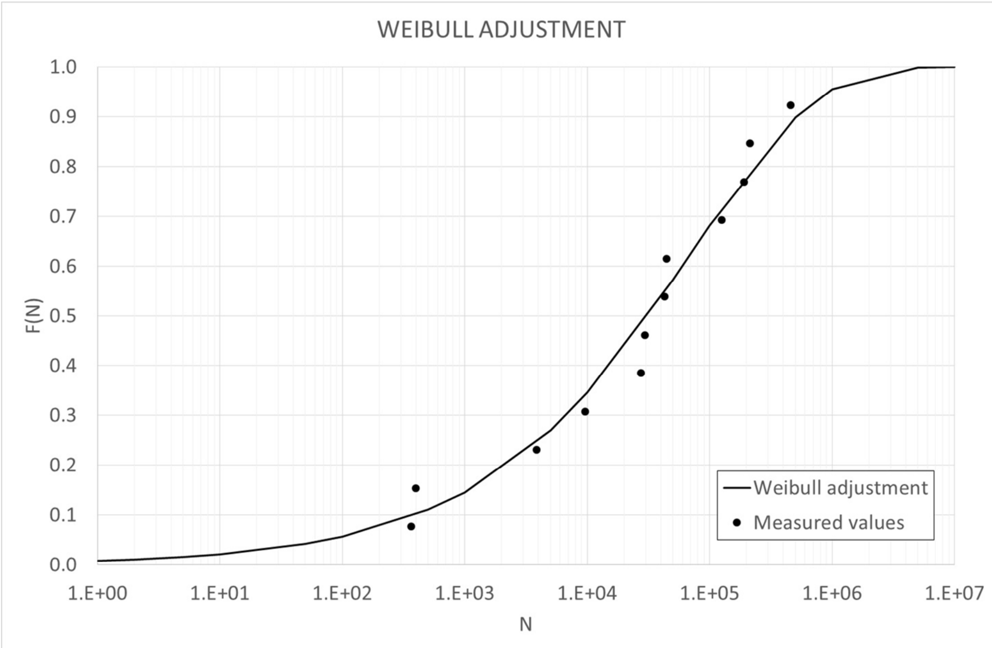

Figure 5: Statistical distribution of fatigue life “N” and Weibull adjustment
310x202mm (120 x 120 DPI)

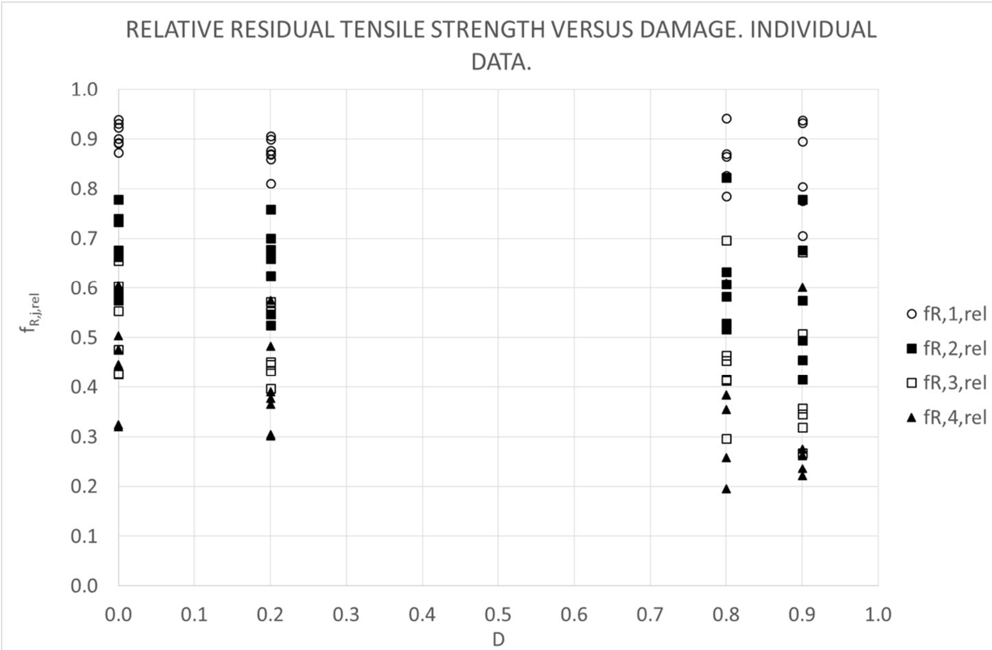

Figure 6: Relative residual tensile strength versus damage. Individual data
310x202mm (120 x 120 DPI)

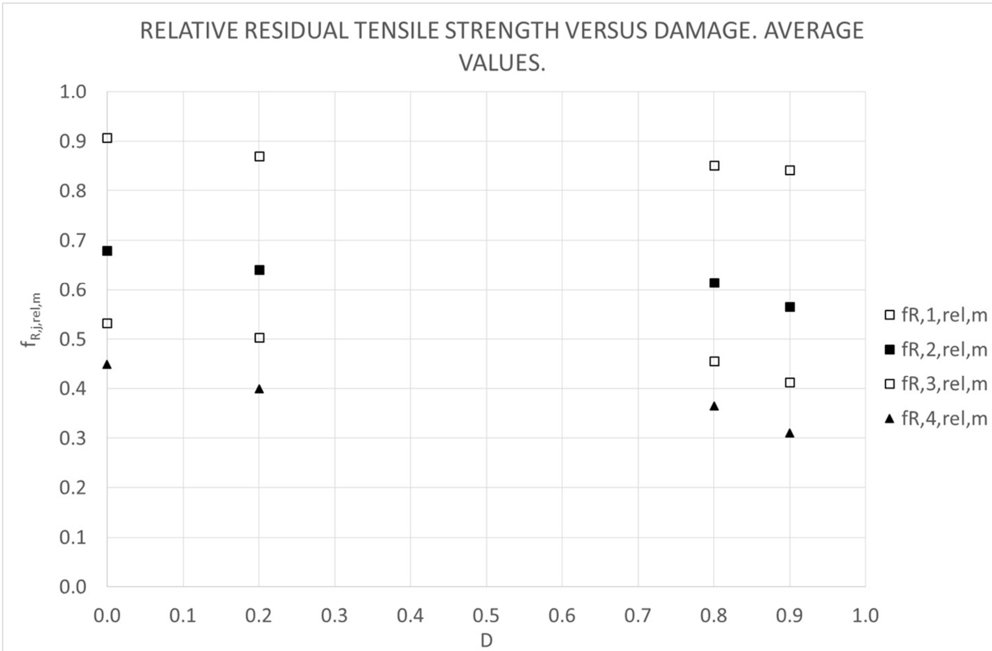

Figure 7: Relative residual tensile strength versus damage. Average values

310x202mm (120 x 120 DPI)

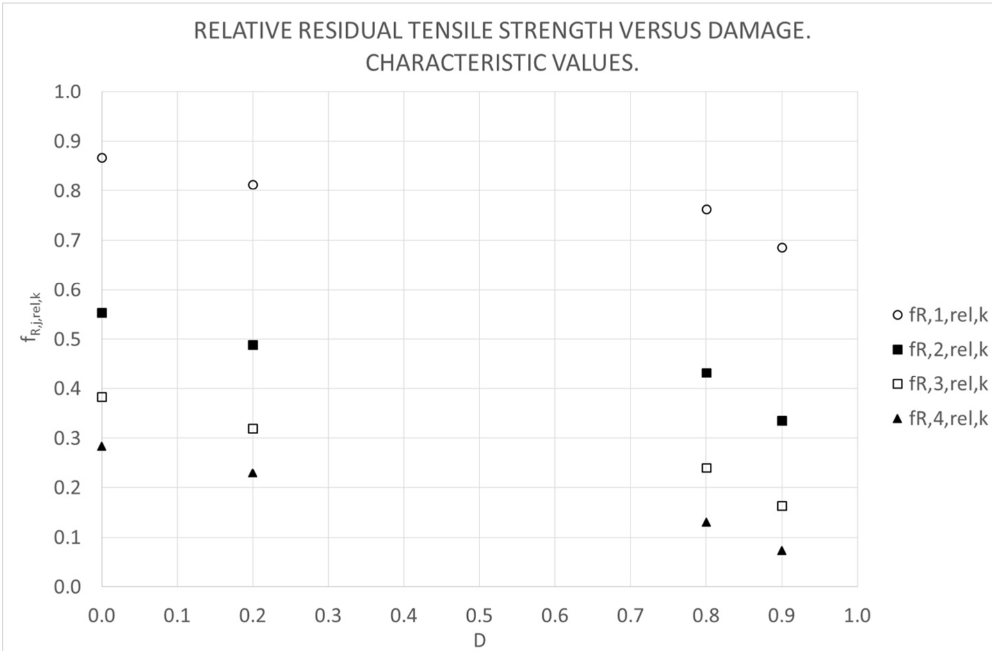

Figure 8: Relative residual tensile strength versus damage. Characteristic values

310x202mm (120 x 120 DPI)

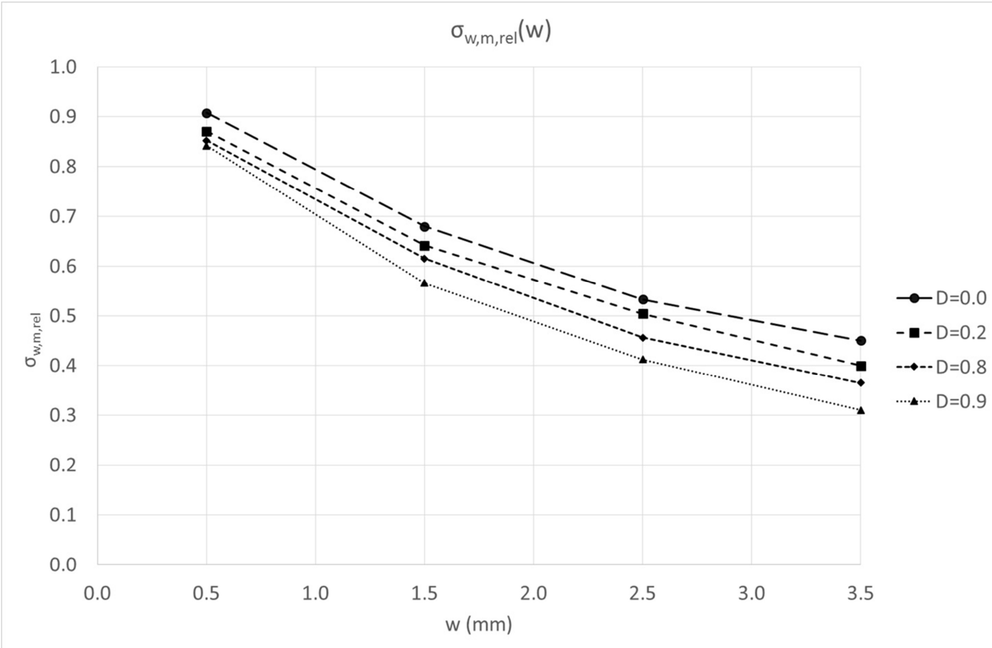

Figure 9: Softening curve relative average stress – crack width
310x202mm (120 x 120 DPI)

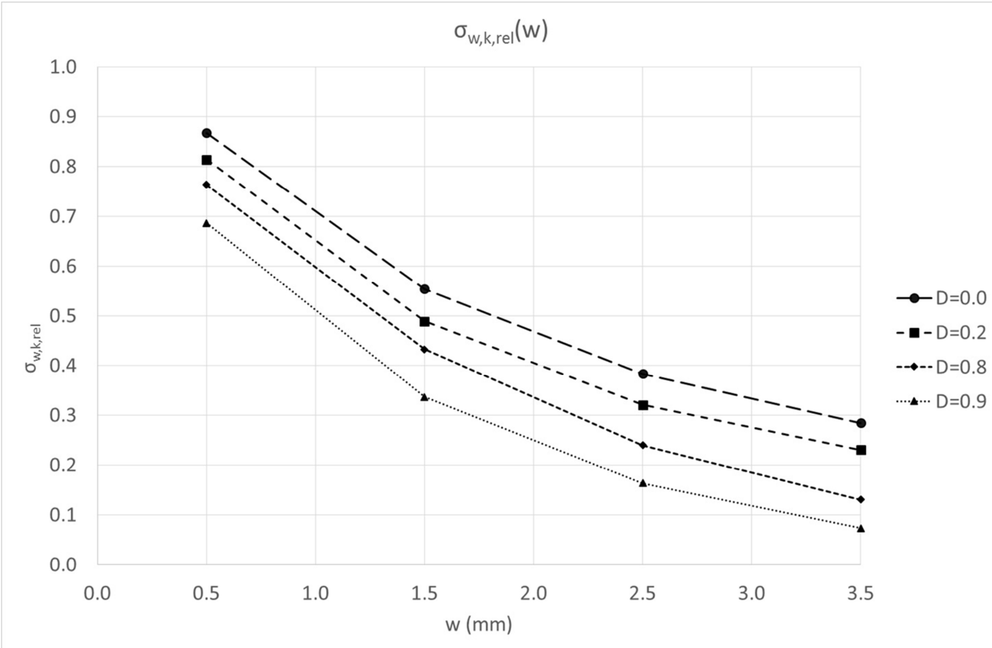

Figure 10: Softening curve relative characteristic stress – crack width
310x202mm (120 x 120 DPI)

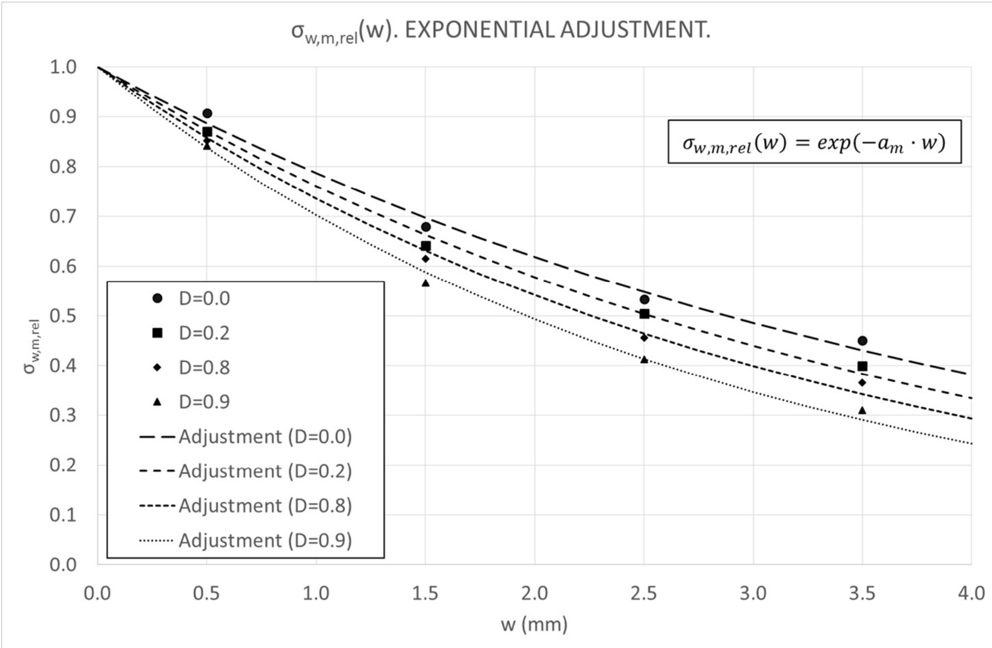

Figure 11: Softening curve relative average stress – crack width. Exponential adjustment
310x202mm (120 x 120 DPI)

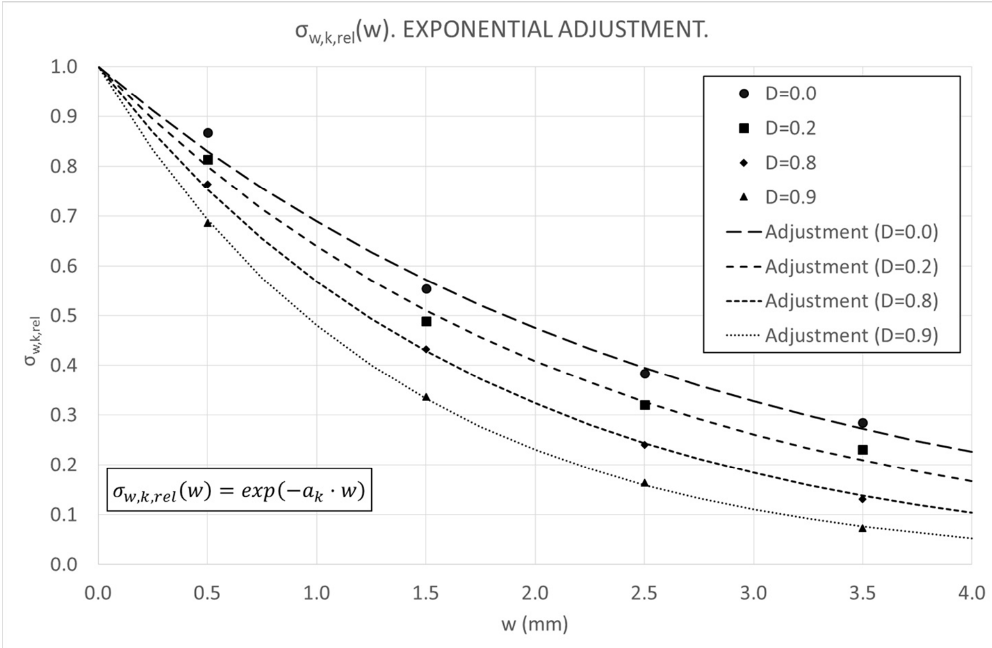

Figure 12: Softening curve relative characteristic stress – crack width. Exponential adjustment
310x202mm (120 x 120 DPI)

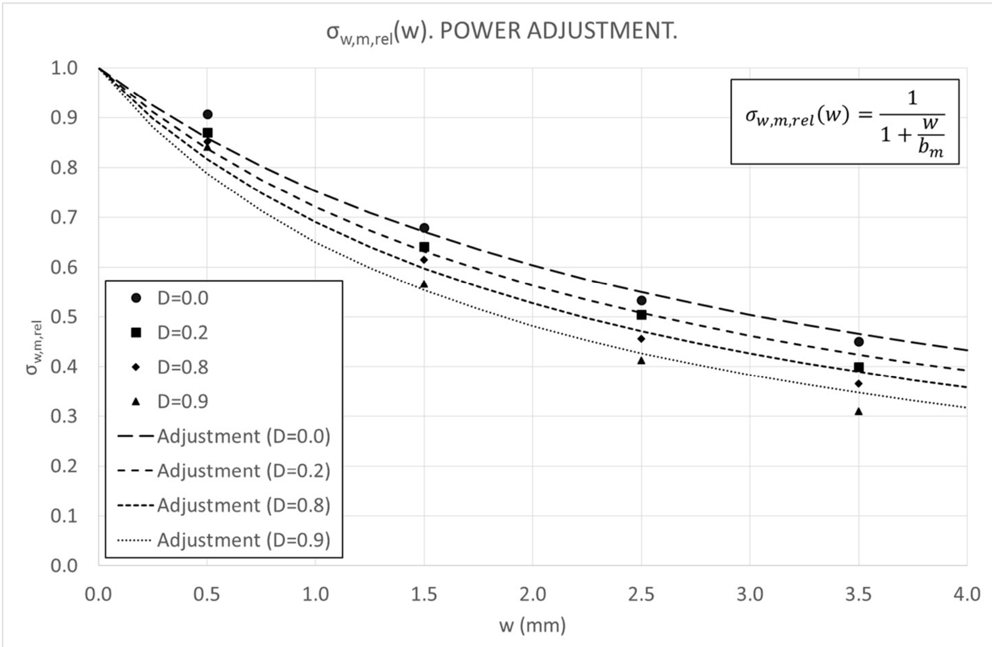

Figure 13: Softening curve relative average stress – crack width. Power adjustment
310x202mm (120 x 120 DPI)

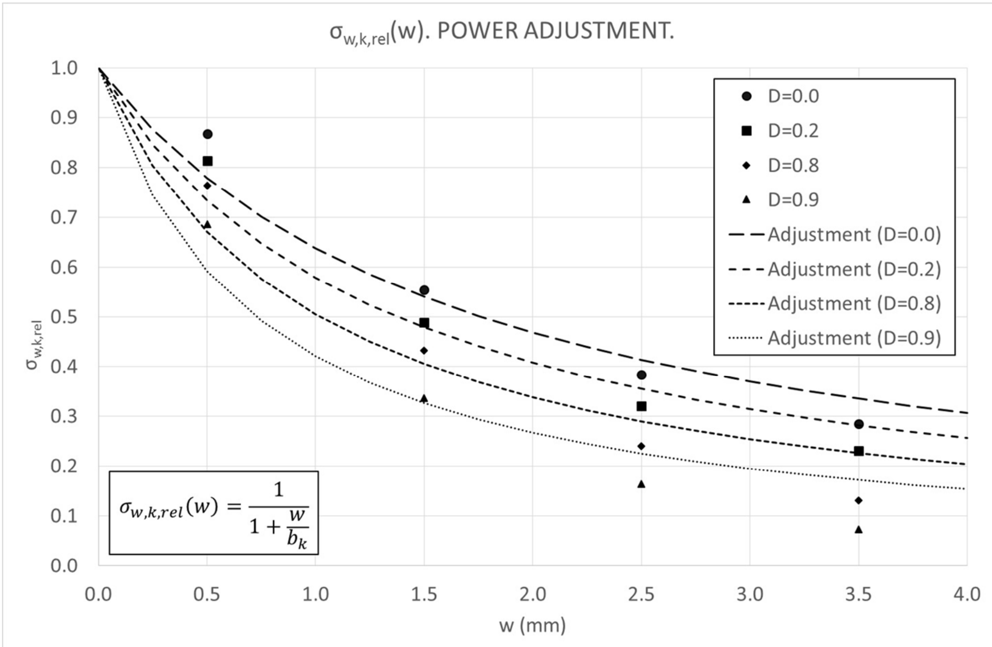

Figure 14: Softening curve relative characteristic stress – crack width. Power adjustment
310x202mm (120 x 120 DPI)

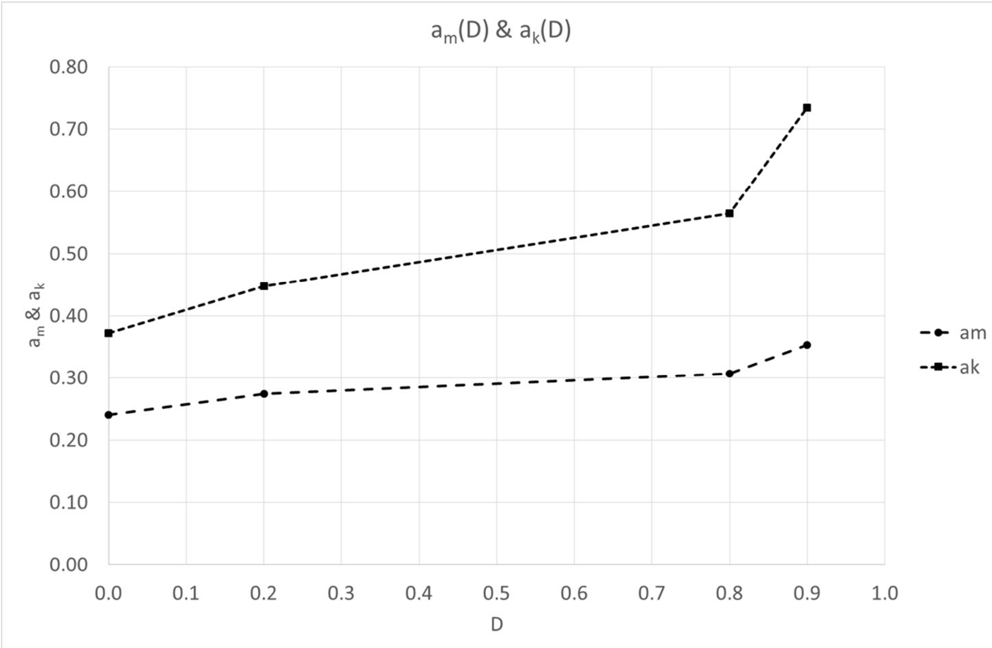

Figure 15: Parameters a_m and a_k versus damage
310x202mm (120 x 120 DPI)

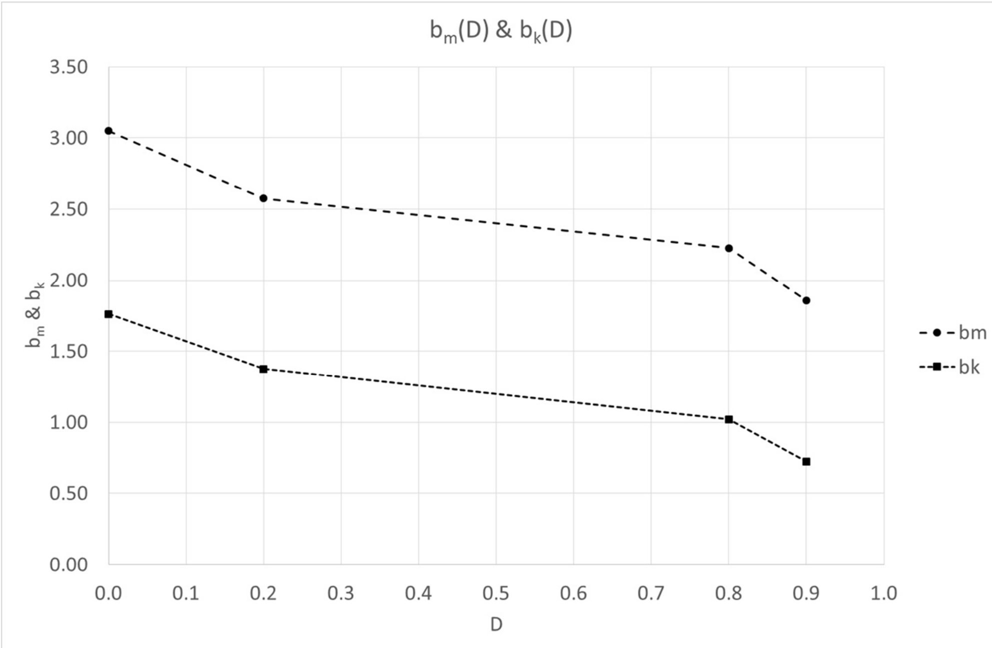

Figure 16: Parameters b_m and b_k versus damage
310x202mm (120 x 120 DPI)

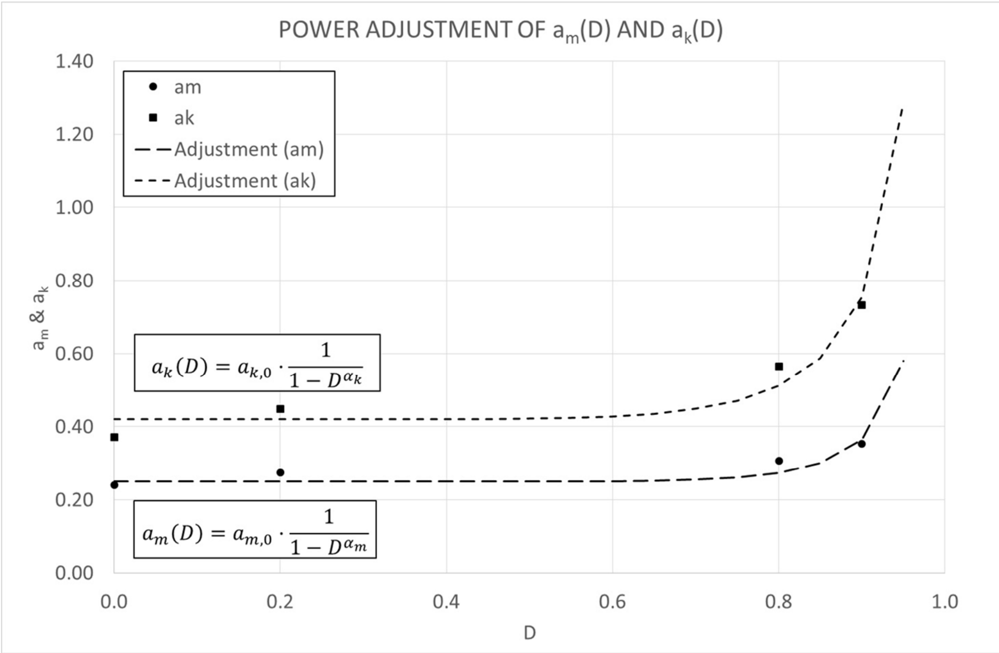

Figure 17: Parameters a_m and a_k versus damage. Power adjustment
310x202mm (120 x 120 DPI)

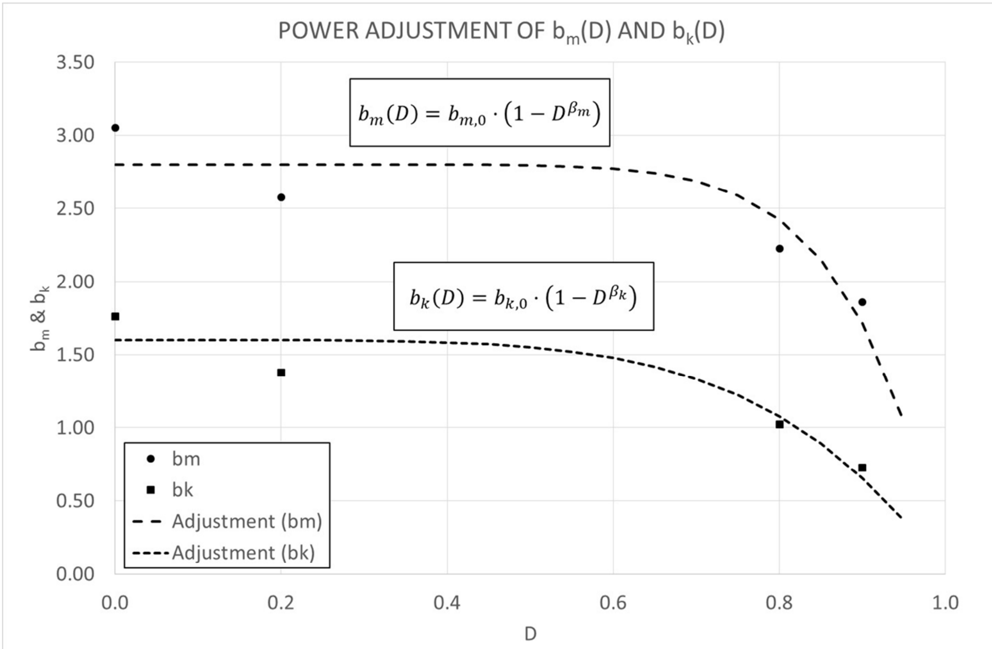

Figure 18: Parameters b_m and b_k versus damage. Power adjustment
310x202mm (120 x 120 DPI)